European Journal of Medicinal Chemistry 46 (2011) 4595–4607

Contents lists available at ScienceDirect

European Journal of Medicinal Chemistry

journal homepage: http://www.elsevier.com/locate/ejmech

Original article

Synthesis, biochemical and molecular modelling studies of antiproliferative azetidinones causing microtubule disruption and mitotic catastrophe

Niamh M. O'Boyle [a,*], Miriam Carr [a], Lisa M. Greene [b], Niall O. Keely [a], Andrew J.S. Knox [c], Thomas McCabe [d], David G. Lloyd [c], Daniela M. Zisterer [b], Mary J. Meegan [a,*]

[a] School of Pharmacy and Pharmaceutical Sciences, Centre for Synthesis and Chemical Biology, Trinity College Dublin, Dublin 2, Ireland
[b] School of Biochemistry & Immunology, Trinity College Dublin, Dublin 2, Ireland
[c] Molecular Design Group, School of Biochemistry & Immunology, Trinity College Dublin, Dublin 2, Ireland
[d] School of Chemistry, Trinity College Dublin, Dublin 2, Ireland

ARTICLE INFO

Article history:
Received 14 April 2011
Received in revised form
13 June 2011
Accepted 22 July 2011
Available online 28 July 2011

Keywords:
Antiproliferative
Azetidinone
β-lactam
Combretastatin
Mitotic catastrophe
Tubulin

ABSTRACT

The structure-activity relationships of antiproliferative β-lactams, focusing on modifications at the 4-position of the β-lactam ring, is described. Synthesis of this series of compounds was achieved utilizing the Staudinger and Reformatsky reactions. The antiproliferative activity was assessed in MCF-7 cells, where the 4-(4-ethoxy)phenyl substituted compound **26** displayed the most potent activity with an IC_{50} value of 0.22 μM. The mechanism of action was demonstrated to be by inhibition of tubulin polymerisation. Cell exposure to combretastatin A-4 and **26** led to arrest of MCF-7 cells in the G2/M phase of the cell cycle and induction of apoptosis. Additionally, mitotic catastrophe for combretastatin A-4 and for **26** was demonstrated in breast cancer cells for the first time, as evidenced by the formation of giant, multinucleated cells.

© 2011 Elsevier Masson SAS. All rights reserved.

1. Introduction

Microtubules are a component of the mitotic spindle and are essential to the mitotic division of cells. Tubulin is an α-β heterodimeric protein which is the main constituent of microtubules [1]. Tubulin is the target of numerous small molecule ligands that act by interfering with microtubule dynamics. These ligands can be broadly divided into two categories – those that inhibit the formation of the mitotic spindle and those that inhibit the disassembly of the mitotic spindle once it has formed [2]. Tubulin has three well-characterised binding sites: the taxane domain, the vinca domain and the colchicine domain and many compounds interact with tubulin at these known sites. Paclitaxel (Taxol, **1**, Fig. 1) binds to tubulin at the taxane site, the vinca alkaloids, including vinblastine (**2**, Fig. 1), bind at the vinca domain and colchicine (**3**, Fig. 1) binds at the colchicine domain. Paclitaxel and vinblastine are in clinical use for many types of cancer [3]. Colchicine and podophyllotoxin are colchicine domain tubulin-binding agents that are not in clinical use due to problems of toxicity. Colchicine was the first drug known to bind to tubulin and inhibit microtubule formation as early at the 1930s [1,4]. Colchicine is not used clinically for the treatment of cancer due to gastrointestinal side-effects [4]. To date, there is no clinically approved drug that binds to the colchicine domain of tubulin and much work continues to be carried out in this area.

The combretastatins are a group of diaryl stilbenes isolated from the stem wood of the South African tree *Combretum Caffrum*. Traditionally, the root bark of *Combretum Caffrum* was powdered and boiled and used by the Zulu tribe as a charm for harming an enemy, but there is no written evidence of use of the plant for treating cancer amongst the indigenous people of Africa [5]. A number of constituent stilbenes were found to inhibit the growth of cancer cells. Combretastatin A-4 (**4,** Fig. 1) demonstrated potent antiproliferative activity against a number of human cancer cell lines including multi-drug resistant cancer cell lines [4]. Stilbene **4** binds to the colchicine domain of tubulin and induces vascular shutdown within tumours [6]. Clinically, a water-soluble prodrug, combretastatin A-4-phosphate (CA4P, fosbretabulin, **5,** Fig. 1) is under evaluation in phase 3 trials for treatment of anaplastic thyroid cancer and in phase 2 trials for non-small cell lung cancer

* Corresponding authors. Tel.: +353 1 8962798; fax: +353 1 8962793.
E-mail addresses: oboyleni@tcd.ie (N.M. O'Boyle), mmeegan@tcd.ie (M. J. Meegan).

0223-5234/$ – see front matter © 2011 Elsevier Masson SAS. All rights reserved.
doi:10.1016/j.ejmech.2011.07.039

Abbreviations

CA-4	Combretastatin A-4
CA-4P	Combretastatin A-4 phosphate
DAMA-colchicine	N-Deacetyl-N-(2-mercaptoacetyl)-colchicine
ER	Estrogen receptor
GTP	Guanidine triphosphate
LDH	Lactate dehydrogenase
mAb	Monoclonal antibody
MTT	3-(4,5-Dimethylthiazol-2-yl)-2,5-diphenyltetrazolium bromide
NMR	Nuclear magnetic resonance
PBS	Phosphate buffered saline
TMCS	Trimethylchlorosilane

and platinum-resistant ovarian cancer [7]. *In vivo*, in isolated tumour systems, vascular shutdown is seen within 20 minutes of the start of infusion of **5**. At 100 mg/kg, rapid and prolonged blood flow shutdown is evident, and both human and murine tumour models show extensive necrosis within 24 h. These effects were also seen at doses between 25 and 1500 mg/kg, indicating the wide therapeutic window [6]. In addition to **5**, a second structurally related prodrug (**6**, ombrabulin, Fig. 1, a water-soluble serine amino acid prodrug) is in clinical trials [7, 8]. A related analogue from the combretastatin A series, combretastatin A-1 diphosphate (**7**, OXi4503, Fig. 1), is being evaluated in hepatic and solid tumours as well as acute myeloid leukemia [7].

Many conformationally restricted analogues of **4** have been reported, the majority of which replace the isomerisable *cis*-double bond in **4** with a heterocycle. Reported heterocyclic CA-4 analogues include imidazole **8** [9], tetrazole **9** [10] and benzoxepin **10** [11] (Fig. 2). The azetidin-2-one (β-lactam) ring [12] is an alternative scaffold for potent non-isomerisable combretastatin analogues (**11**–**13**, Fig. 2) [13–16]. Having previously investigated comprehensive structure-activity relationships of these series with a phenyl substituted ring at the 3-position of the azetidinone ring, it was of importance to extend the SAR by investigating a range of aryl substituents at the 4-position. It was also valuable to further characterise the biochemical effects of both **4** and these β-lactam compounds. Herein we report novel findings for **4** and related β-lactam analogues in MCF-7 breast cancer cells.

2. Results and discussion

2.1. Chemistry

The design of this series of compounds incorporated a 3,4,5-trimethoxyphenyl ring at the N-1 position of the β-lactam ring, previously demonstrated to be the optimal substituent at this position [15]. This mimics the A-ring of **4** (Fig. 1). The choice of substituents at the 4-position was based on previously reported potent derivatives of **4**. The first step in the synthesis of the required β-lactams was the formation of the imine precursors **14**–**25**. This is achieved by condensation of the appropriately substituted benzaldehydes and anilines (Schemes 1 and 2). The desired imines were obtained in high yields. Synthesis of β-lactams **27**–**33** and **35**–**37** was carried out using the Staudinger reaction with *in situ* generation of a ketene and subsequent reaction with the appropriately substituted imine (method I, Schemes 1 and 2). A modified Staudinger method (method II, Scheme 1) requiring overnight reaction was used to obtain bromo-containing β-lactam **34** as method I was unsuccessful [17]. Where the appropriate α-bromoacetate precursor was available, the Reformatsky reaction was used for azetidinone synthesis (**26**, Scheme 1, method III). The stereochemistry of the β-lactam product obtained can vary depending on numerous factors, including the reaction conditions, the order of addition of the reagents and the substituents present on both the imine and on the acid chloride [18–20]. The X-ray crystal structure of β-lactam **26** shows the *trans* arrangement for protons H-3 and H-4 of the β-lactam ring, with J values of 2 Hz (Fig. 3). This *trans* stereochemistry was observed for all β-lactam compounds synthesised with phenyl rings directly attached to

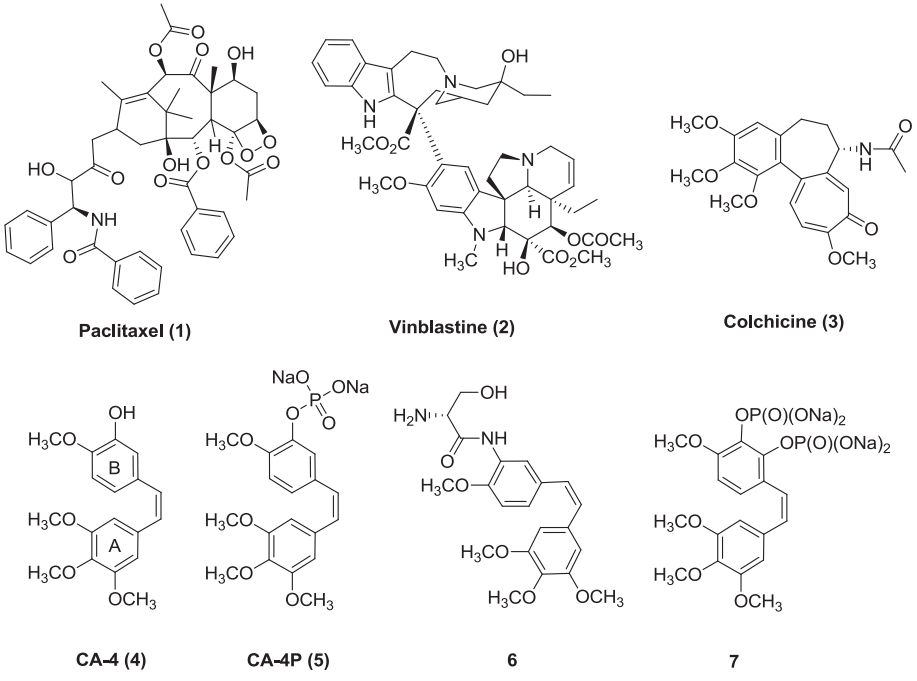

Fig. 1. Tubulin binding agents.

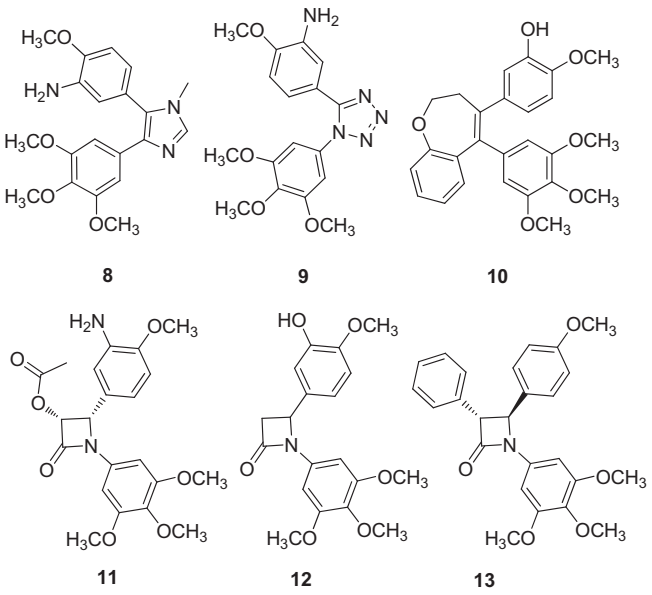

Fig. 2. Heterocyclic analogues of **4**.

positions 3 and 4 of the ring, as evidenced by the coupling constants, $J_{3,4} \simeq 2$ Hz. No *cis* isomers were detected in this series, probably due to steric hindrance between the 3- and 4-positions of the azetidin-2-one ring.

β-Lactams **38**, **39** and **40** are diphenyl substituted at the 4-position of the azetidinone ring. The imine precursors, obtained from the appropriately substituted benzophenones, could not be isolated under normal reflux conditions in ethanol. It has been noted previously that it is more difficult to synthesise Schiff bases from ketone precursors such as acetophenone and benzophenone than from less sterically hindered aldehydes such as *para*-methoxybenzaldehyde. Anhydrous conditions, lengthy reaction times, high temperatures and the use of activated molecular sieves are normally required [21]. A number of different reaction conditions were attempted for these compounds. Reaction of benzophenones with 3,4,5-trimethoxyaniline did not proceed when using 4 Å molecular sieves, reflux conditions and anhydrous toluene [22]. Refluxing with benzene, molecular sieves and sodium bicarbonate also did not yield any of the desired imine [23]. An alternative, one-pot preparation of β-lactams using titanium (IV) chloride was explored [24]. This method uses half an equivalent of $TiCl_4$ in the condensation of the appropriate aniline and benzophenone using tri-*n*-butylamine as the base. Subsequent reaction with the appropriate acid chloride without isolation of the intermediate imine yielded the desired β-lactams **38**, **39** and **40** in low yields (Scheme 3).

2.2. Pharmacology and biochemical results

2.2.1. Antiproliferative activity in breast cancer cells

Compounds **26**–**40** were screened for their antiproliferative activity in the ER expressing MCF-7 human breast cancer cell line using the MTT assay [25]. The drug concentration required to inhibit the cell growth by 50% (IC_{50}) was determined and the results are displayed in Table 1. Additional screening using the ER independent MDA-MB-231 human breast cancer cell lines was carried out for selected analogues.

The antiproliferative activity of the 3-phenyl substituted β-lactams in MCF-7 and MDA-MB-231 breast cancer cells (Table 1) are in general agreement with our previously reported results obtained for a series of 3-unsubstituted β-lactam compounds [14]. β-Lactam **13** was chosen as the lead compound due to both its synthetic accessibility and the potential to examine a number of related analogues to examine the structure-activity relationships of derivatives with variations at the 4-position of the β-lactam ring. 4-Ethoxy derivate **26** was the most potent compound in this series in MCF-7 cells with an IC_{50} value of 0.22 μM. This is a decrease in activity of approximately 10-fold compared to **13**, and is consistent with previously reported ethoxy-substituted combretastatin derivatives [26]. Surprisingly **27**, the 4-fluoro compound displays submicromolar activity which is not shown in a related 3-unsubstituted compound previously reported [14]. However, potent fluoro-containing analogues of **4** are known [27]. The 4-dimethylamino substituted compound **28** and 3,4-dimethoxyphenyl compound **33** also exhibit submicromolar activity. The inclusion of the two trimethoxy ring systems (as in compounds **29**, **30**, **31** and **32**) gives less active compounds with antiproliferative values in the high micromolar range regardless of the substitution pattern of the methoxy groups at position 4. A bromine-containing analogue (**34**, $IC_{50} = 1.42$ μM) was of interest as a derivative of **4** which replaced the hydroxy group of Ring B with a bromide substituent was reported to have moderate activity in a range of cell lines [28]. In our series, this compound was not as potent as either the lead compound **13** or **26**. However, this compound has the potential to be used as an intermediate in the synthesis of further boronic acid β-lactams, as has been reported for potent boronic acid bioisosteres of **4** [29]. The 2-naphthalene moiety has been demonstrated to be good surrogate for the B-ring of the combretastatin series [30], and the equivalent β-lactam **35** containing a 2-naphthalene ring at the 4-position shows submicromolar activity with an IC_{50} value of 0.44 μM.

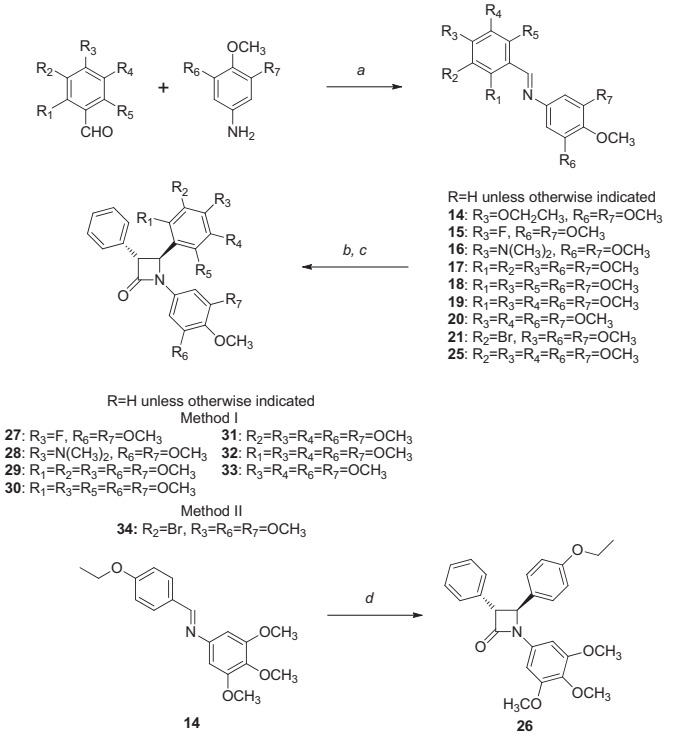

Scheme 1. Reagents and conditions: (a) ethanol, reflux, 3 h; (b) method I: $C_6H_5CH_2COCl$, $(CH_3CH_2)_3N$, CH_2Cl_2, 3 h, reflux; (c) method II: $C_6H_5CH_2COCl$, $(CH_3CH_2)_3N$, triphosgene, CH_2Cl_2, overnight; (d) method III: ethyl-α-bromophenylacetate, zinc, TMCS, benzene, microwave (only one enantiomer of β-lactam compounds illustrated for clarity).

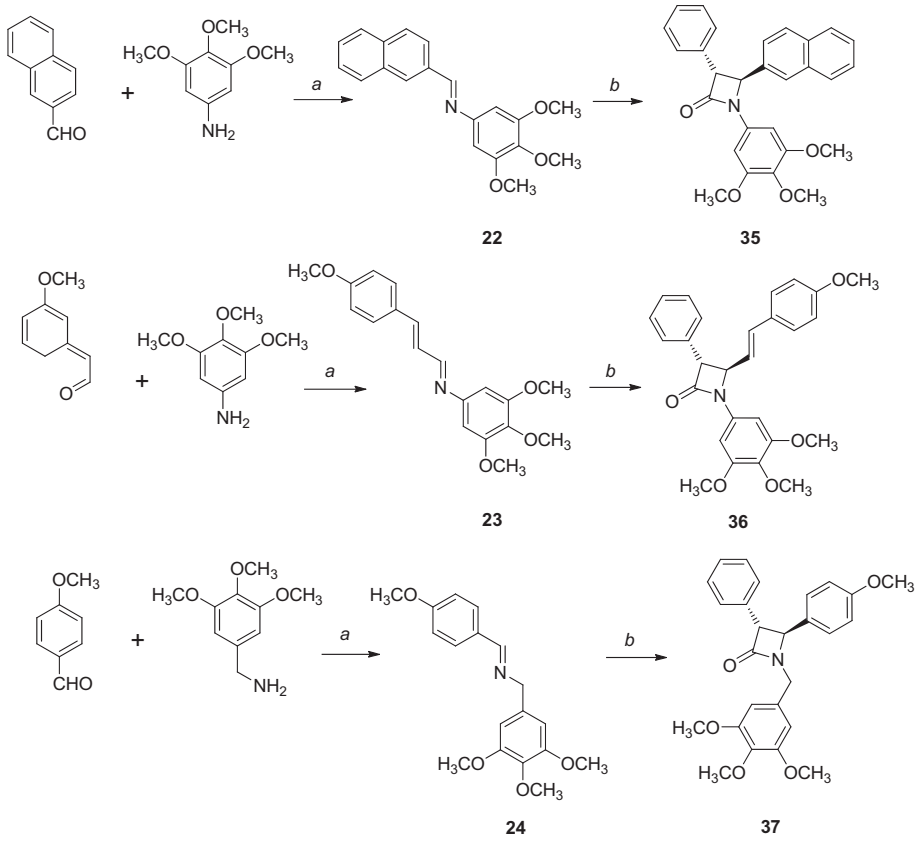

Scheme 2. Preparation of β-lactams **35**, **36** and **37** via the Staudinger reaction. Reagents and conditions: (a) ethanol, reflux, 3 h; (b) $C_6H_5CH_2COCl$, $(CH_3CH_2)_3N$, CH_2Cl_2, reflux, 3 h (only one enantiomer of β-lactam compounds illustrated for clarity).

Other aryl substituent variations at the C-4 position were also examined. Removal of the direct attachment of the phenyl ring to the β-lactam core results in reduction of antiproliferative effect by a factor of 100 (vinyl analogue **36** has an IC_{50} value of 1.99 μM compared to 0.034 μM for **13**). This is also true of the N-1 position, where a methylene spacer introduced in compound **37** between the core β-lactam ring and the trimethoxyphenyl ring led to a decrease in activity by over a thousand-fold (IC_{50} value of 38.6 μM compared to 0.034 μM for **13**). The introduction of the two phenyl rings at the C-4 position leads to a small decrease in antiproliferative activity for **39** and **40**, both of which contain methoxy groups on one or both phenyl rings, showing antiproliferative effects at sub-micromolar concentrations. Compound **38**, without methoxy groups at the 4-position, is less potent ($IC_{50} = 3.84$ μM).

This series of analogues did not display submicromolar anti-proliferative activity equipotent with either **4** or **13** in MDA-MB-231 breast cancer cells, with the exception of compounds **26** and **33**. Compound **26** had an IC_{50} value of 0.83 μM while 4-(3,4-dimethoxyphenyl) substituted β-lactam **33** had an IC_{50} value of 0.53 μM which was nearly 7-fold less potent than **13** (Table 2).

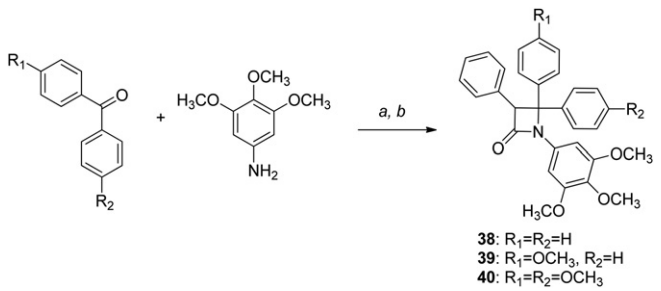

Scheme 3. Preparation of 4,4-diphenyl substituted β-lactams **38**–**40**. Reagents and conditions: (a) $TiCl_4$, anhydrous toluene, tri-*n*-butylamine, 18 h (b) Tri-*n*-butylamine, $C_6H_5CH_2COCl$, reflux, 8 h.

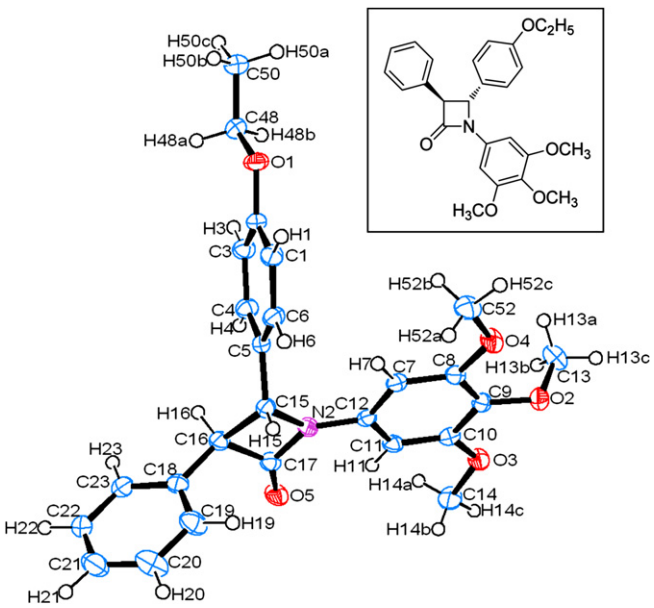

Fig. 3. Ortep representation of the crystal structure of **26** with displacement ellipsoids plotted at 50%.

Table 1
Antiproliferative effects of combretastatin β-lactam analogues **26**–**40** in MCF-7 cells.

Compound	IC_{50} value (μM)[a]
26	0.22 ± 0.1
27	0.35 ± 0.1
28	0.85 ± 0.9
29	1.12 ± 1.2
30	18.7 ± 12
31	69.8 ± 82
32	46.9 ± 18
33	0.46 ± 0.4
34	1.42 ± 0.9
35	0.44 ± 0.08
36	1.99 ± 1.04
37	38.6 ± 16
38	3.84 ± 2.2
39	0.43 ± 0.17
40	0.64 ± 0.10
4[b]	0.005 ± 0.002
13 [15]	0.034 ± 0.02

[a] IC_{50} values are half maximal inhibitory concentrations required to block the growth stimulation of MCF-7 cells. Values represent the mean ± S.E.M (error values × 10^{-6}) for at least three experiments performed in triplicate.
[b] The IC_{50} value obtained for **4** in this assay is 0.005 μM for MCF-7 which is in good agreement with the reported values for **4** using the MTT assay on human MCF-7 breast cancer cell line [35,44–46].

The cytotoxicity of selected analogues at 10 μM was determined using an LDH assay. The range of cytotoxicity in MCF-7 cells was between 3% for **33** and 10.4% cell death for dimethylamino-containing analogue **28**. These values are comparative to the percentage of cell death of 5.5% at 10 μM observed for **4** in MCF-7 cells. In MDA-MB-231 cells, cytotoxicity at 10 μM ranged from 0% (analogues **27**, **30**, **31**, **32** and **33**) to 6.1% (compound **29**), again falling in the same low percentage range as **4** (4.3%). The cytotoxicity for the most potent compound, **26**, was 5.4%. This confirms previous work in normal murine epithelial cells that both **4** and β-lactam derivatives are minimally cytotoxic to non-proliferating cells [15,16].

2.2.2. Tubulin polymerization and immunofluorescence

β-Lactam **26** was chosen for further study on the basis of its potent antiproliferative activity in MCF-7 cells, together with an assessment of its drug-like properties via a Tier 1 profiling screen. Compound **26** satisfies Lipinski's 'rule of five' for drug-like properties e.g. molecular weight (433) is less than 500, the number of oxygen/nitrogen atoms is less than 10, the number of hydrogen bond donors is less than 5 and the cLog *P* value of 3.72 (<5), imply that this is a moderately lipophilic–hydrophobic drug and is a suitable candidate for further investigation (in addition to predictions of permeability, metabolic stability, Pgp substrate status, blood-brain barrier partition, plasma protein binding and human intestinal absorption properties which indicated the suitability of these compounds for further development).

In this study, we investigated the tubulin-targeting properties of **26** by a turbidity assay and confocal microscopy. As expected, **26** (10 μM) completely inhibited the assembly of tubulin in a cell free tubulin turbidity assay in a similar manner to that previously reported for **4** (Fig. 4) thus confirming that the target of this series of compounds is tubulin. In an attempt to identify the cellular effects that may be relevant to the antiproliferative activity of **26**, we evaluated their activity on the alteration of the microtubule network by tubulin immunostaining, comparing it to that of **4**. Confocal analysis of MCF-7 cells stained with α-tubulin mAb demonstrated a well organised microtubular network in control cells (Fig. 5). Exposure to **4** (100 nM) or **26** (500 nM) for 16 h led to a complete loss of microtubule formation consistent with depolymerised microtubules (Fig. 5). Additionally, cells treated with **4** and **26** increased in cell size and contained multiple micronuclei – a phenomenon described as mitotic catastrophe. Mitotic catastrophe is a type of programmed cell death in response to DNA damage, characterised by giant multinucleated cells [31]. These findings are in agreement with previously published studies, where **5** induced mitotic catastrophe in chronic lymphocytic leukemia cells [32]. Similarly, **4** and a combretastatin derivative induced mitotic catastrophe dependent on spindle checkpoint and caspase-3 activation in non-small cell lung cancer cells [33]. Mitotic catastrophe has also been demonstrated for **4** and related derivatives in both human endothelial cells (HUVEC) and human lung carcinoma cells (H460) [34,35]. Taken together, these results confirm tubulin as the molecular target of this series of β-lactam combretastatin derivatives and demonstrate mitotic catastrophe in MCF-7 breast cancer cells for **4** and **26** for the first time.

Table 2
Antiproliferative effects of combretastatin β-lactam analogues in MDA-MB-231 cells.

Compound	IC_{50} (μM)[a]
26	0.83 ± 0.002
27	1.14 ± 0.2
28	5.66 ± 2.4
29	1.96 ± 0.09
30	5.74 ± 4.9
31	65.6 ± 2.6
32	38.9 ± 12
33	0.53 ± 0.02
4[b]	0.043
13 [15]	0.078 ± 0.04

[a] IC_{50} values are half maximal inhibitory concentrations required to block the growth stimulation of MDA-MB-231 cells. Values represent the mean ± S.E.M (error values × 10^{-6}) for at least three experiments performed in triplicate.
[b] The IC_{50} value obtained for **4** in this assay is 0.043 μM for MDA-MB-231 which is in good agreement with the reported values for **4** using the MTT assay on the human MDA-MB-231 breast cancer cell line [47,48].

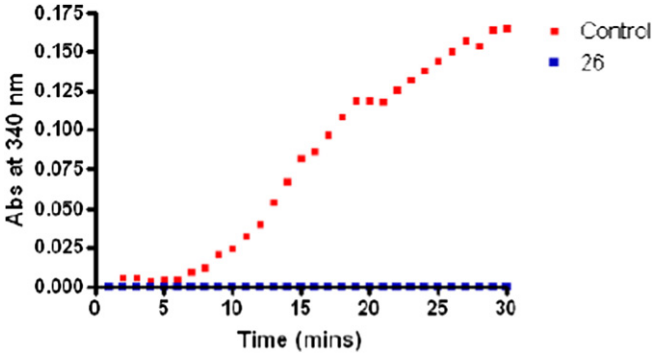

Fig. 4. Tubulin polymerization for **26** (blue squares) and ethanol (vehicle control, red squares). Effects of compound **26** (10 μM) on *in vitro* tubulin polymerization. Purified bovine tubulin and GTP were mixed in a 96-well plate. The reaction was started by warming the solution from 4 °C to 37 °C. Ethanol (1%v/v) was used as a vehicle control. The effect on tubulin assembly was monitored in a Spectramax 340PC spectrophotometer at 340 nm at 30 s intervals for 60 min at 37 °C. The graph shows one representative experiment. Each experiment was performed in triplicate (For interpretation of the references to colour in this figure legend, the reader is referred to the web version of this article.)

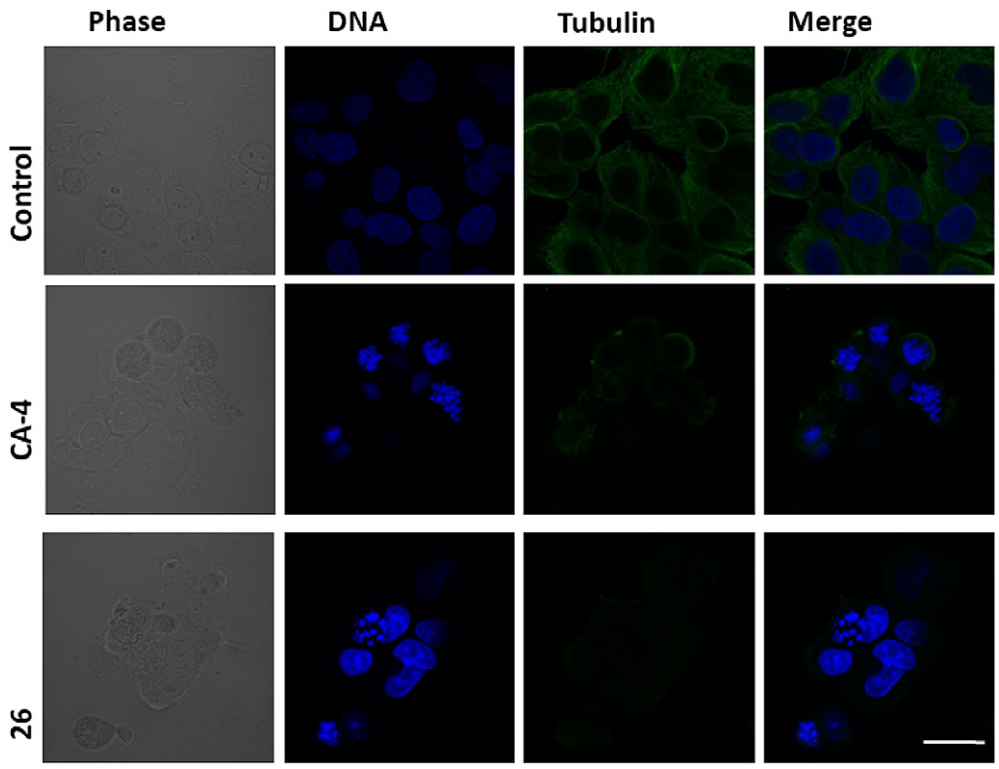

Fig. 5. CA-4 (**4**) and β-lactam **26** depolymerise the microtubule network of MCF-7 cells resulting in mitotic catastrophe. MCF-7 cells were treated with vehicle [1% ethanol (v/v)], CA-4 (**4**) [100 nM] or **26** (500 nM) for 16 h. Cells were fixed in methanol and stained with α-tubulin mAbs (green) and counterstained with DAPI (red). Images were captured by confocal microscopy coupled with OLYMPUS FLUOVIEW software. Bar equal to 40 μm. Representative confocal micrographs of three separate experiments are shown (For interpretation of the references to colour in this figure legend, the reader is referred to the web version of this article.)

2.2.3. Analysis of DNA content by flow cytometry

We next examined the effect of **4** and β-lactam **26** on the cell cycle of MCF-7 cells by flow cytometric analysis of propidium iodide stained cells. After 48 h, both **4** and **26** induced a significant increase in the percentage of cells in the G_2M phase of the cell cycle (52% and 47.5% respectively compared to 19.7% in untreated cells, $P = 0.02$) together with a significant increase in apoptosis as determined by quantification of the sub-G1 population of cells (9.4% and 13.97% respectively compared to 1.65% in untreated cells) (Table 3 and Fig. 6).

2.3. Structural studies of β-lactam compound 26 in the colchicine-binding site of tubulin

The proposed mode of binding of β-lactam **26** was investigated by virtual molecular docking using a published crystal structure of DAMA-colchicine (**41**) bound to the colchicine domain of αβ-tubulin [36]. Fig. 7 illustrates the key interactions observed for **41** in the active site of tubulin. It is clear that **41** appears to bind to the interface of the αβ heterodimer of tubulin. The key contacts involved have been described by Knossow et al. with the trimethoxy A-ring of **41** interacting with Cys241 [36]. Crosslinking studies with trimethoxy-substituted A-rings with more reactive groups have previously shown the importance of Cys241 in the binding process [36,37]. A similar binding orientation is observed for the trimethoxyphenyl A-rings of **41** and **26** (Fig. 7). The positioning of the trimethoxy substituents of the A-rings differ slightly due to the 3D conformation of the molecule but both can still interact favorably with Cys241 to provide the anchoring interaction in the binding site. These binding parallels may rationalize the antiproliferative potency observed for **26**. The C-ring at the 3-position of the β-lactam is observed to fill the pocket of tubulin more optimally than in the case of colchicine. This binding orientation differs from that previously observed for a related series of β-lactams, where the aryl ring at the C-4 position of the β-lactam filled the space occupied by the C-ring of colchicine [15,16].

Hydrogen bonding between sulfur and Ser178 is also depicted in Fig. 7 in both the co-crystal of **41** and also the docked complex of **26** which uses oxygen as a H-bond acceptor in this case. It is likely that a steric clash between the longer ethoxy side chain and the residues in the binding site contributes to the changed binding conformation in comparison to **3**, **4** and **13** where the 3-hydroxy-4-methoxyphenyl ring (or C-4 4-methoxyphenyl ring in the case of **13**) occupies the space now occupied by the C-3 phenyl ring of **26**. The difference in positioning of the ethoxy side chain of **26** and the methoxy group of the C-ring of **41** may be significant for observed antiproliferative activity of **26** in combretastatin-resistant cell lines (data not shown).

Table 3
Flow cytometric analysis of both cell death (sub-G1) and the cell cycle in MCF-7 cells exposed to **4** and β-lactam **26**.[a]

Compound	Sub-G_1 (%)	G_1 (%)	S (%)	G_2/M (%)	Polyploidy (%)
Untreated	1.65 ± 0.38	60.22 ± 3.1	8.77 ± 0.9	19.72 ± 1.2	8.83 ± 2.5
Ethanol (1% v/v)	1.26 ± 0.2	63.76 ± 4.1	9.05 ± 1.6	18.31 ± 1.7	7.01 ± 3.8
4	9.43 ± 2.1	23.57 ± 5.9	10.66 ± 2.4	52.02 ± 5.9	8.36 ± 1.9
26	13.97 ± 3.2	21.18 ± 3.0	9.49 ± 0.27	47.53 ± 4.7	7.40 ± 2.2

[a] Cell cycle analysis of MCF-7 cells untreated or treated with vehicle control (1% (v/v) ethanol), **4** (100 nM) or **26** (500 nM) for 48 h. % MCF-7 cells in each cell cycle phase are shown after exposure to compounds **4** or **26** for 48 h. Cells were analysed with the FACScan flow cytometry. Cells in the sub-G1 peak are indicative of apoptotic cells. Results show a typical experiment which has been repeated three times. Values represent the mean ± standard deviation for three experiments.

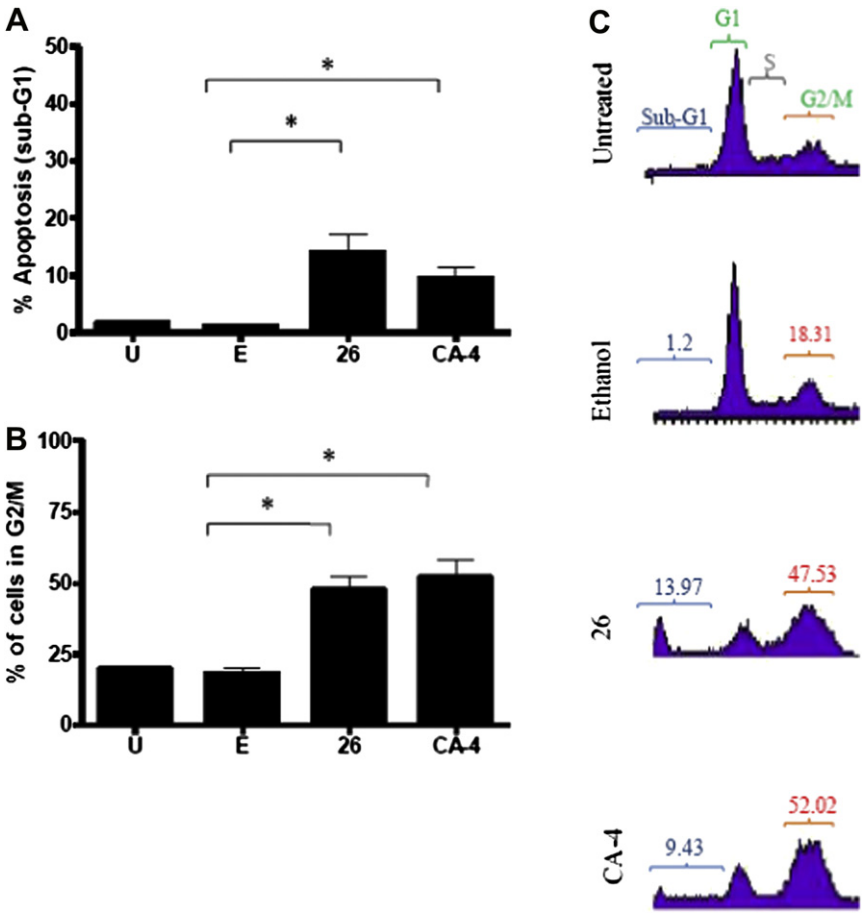

Fig. 6. Effect of **4** and **26** on the cell cycle. MCF-7 cells were left untreated (U) or treated with vehicle (E) [1% ethanol (v/v)], CA-4 (**4**) [100 nM], **26** [500 nM] for 48 h. Percentages of (A) G_2M arrested cells and (B) apoptotic (sub-G1) are indicated. Values represent the mean ± SEM for at least three separate experiments. $^*P < 0.05$. C, representative DNA profiles are shown and mean percentage of cells in sub-G1 and G_2M are indicated.

Structurally, similarity between the common features of **3**, **4** and antiproliferative β-lactams has been demonstrated. Of particular note is that the crystal structures of **4** [38], **5** [28], **13** [15] and **26** show non-coplanar ring systems. In the crystal structure of the β-lactam **26** (Fig. 3), the distance between the centroid of the C-3-phenyl and N-1-phenyl rings is 7.338 Å, in comparison to 6.193 Å for the distance between the centroids of C-3 and C-4 phenyl rings and 5.146 Å between the N-1 and C-4 phenyl rings (Fig. 8). The comparative distance between the centroids of the A- and C-rings of the co-crystal structure of **41** is 4.516 Å. Surprisingly, the equivalent distance between the centroids of A- and B-rings of **4** (5.191 Å) is closer in distance to that between N-1 and C-4 of β-lactam compound **26**, but despite this, the preferred orientation of **26** in the molecular docking with tubulin showed overlay of the N-1 and C-3 rings of **26** with the A- and B-rings of **41**.

3. Conclusion

A novel series of antiproliferative agents are described. Structural and molecular modelling studies rationalize the observed antiproliferative activities. Interesting effects on microtubule dynamics were observed both for **4** and β-lactam derivative **26**, including mitotic catastrophe in MCF-7 breast cancer cells observed for the first time. MCF-7 breast cancer cells treated with **4** and **26** undergo cell death both through microtubule disorganization and mitotic catastrophe, as demonstrated by the presence of giant multinucleated cells. These observations suggest that the activities of **4** and **26** in MCF-7 cells might not be related solely to a microtubule-damaging mechanism and that additional mechanisms involved in mitosis control should be considered. The unusual effects of these compounds are significant and are under further investigation.

4. Experimental protocols

4.1. Chemistry

All reagents were commercially available and were used without further purification unless otherwise indicated. Toluene was dried by distillation from sodium and stored on activated molecular sieves (4 Å) and dichloromethane was dried by distillation from calcium hydride prior to use. IR spectra were recorded as thin films on NaCl plates or as KBr discs on a Perkin-Elmer Paragon 100 FT-IR spectrometer. ^1H and ^{13}C NMR spectra were obtained on a Bruker Avance DPX 400 instrument at 20 °C, 400.13 MHz for ^1H spectra, 100.61 MHz for ^{13}C spectra, in $CDCl_3$ (internal standard tetramethylsilane) by Dr. John O'Brien and Dr. Manuel Ruether in the School of Chemistry, Trinity College Dublin. High resolution accurate mass determinations for all final target compounds were obtained on a Micromass time of flight mass spectrometer (TOF) equipped with electrospray ionization (ES) interface operated in the positive ion mode at the High Resolution Mass Spectrometry Laboratory by Dr. Martin Feeney in the School of Chemistry, Trinity College Dublin. Elemental analysis was carried out in the microanalytical laboratory at University College Dublin, Belfield, Dublin 4. Thin layer chromatography was performed using Merck Silica gel

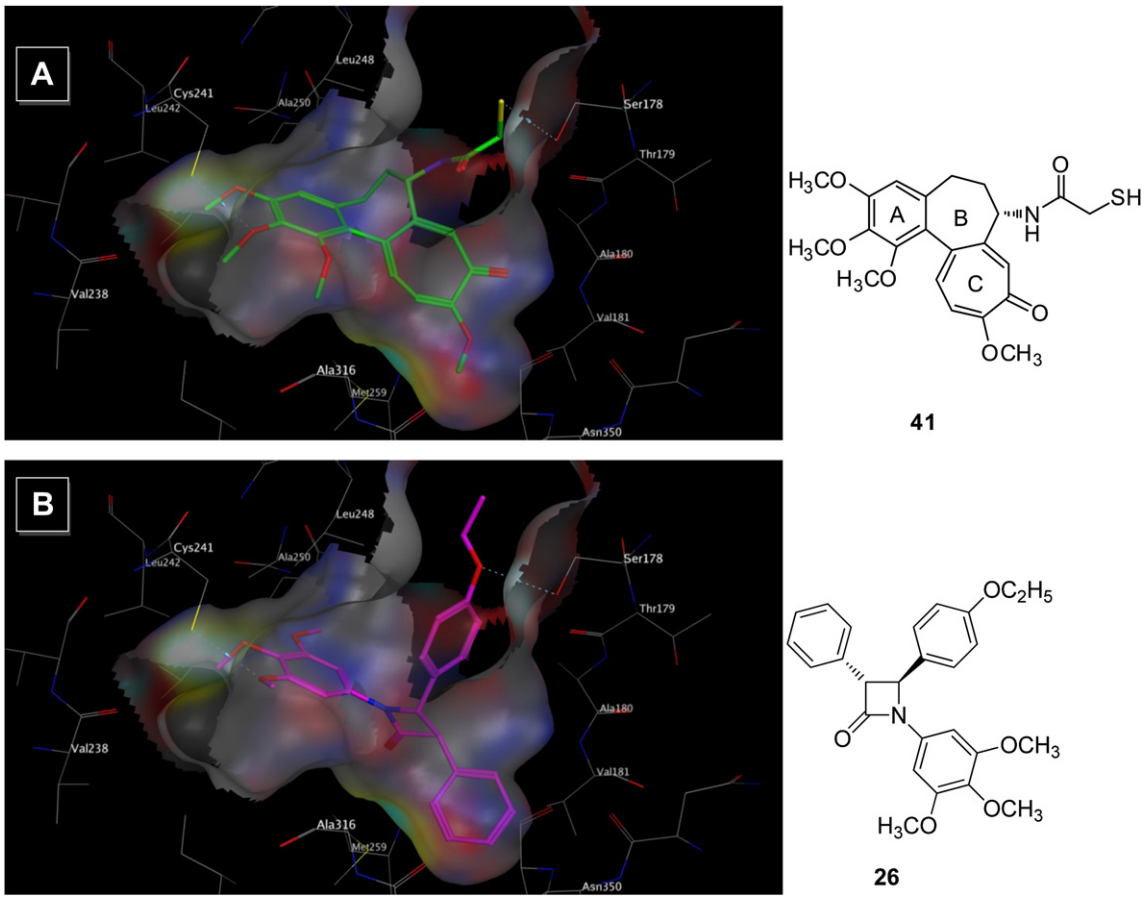

Fig. 7. The crystal structure of tubulin with (A) DAMA-colchicine **41** and (B) docked X-ray of compound **26** in the same active site. Docked pose of **41** and β-lactam **26** in the colchicine-binding site of tubulin (PDB entry 1SA0). Hydrogens are not shown for clarity. Coloured by atom: Green (colchicine carbon); Pink (β-lactam carbon); red (oxygen); blue (nitrogen). Residue numbers are those used by Ravelli et al. [36] (For interpretation of the references to colour in this figure legend, the reader is referred to the web version of this article.)

60 TLC aluminium sheets with fluorescent indicator visualizing with UV light at 254 nm. Flash chromatography was carried out using standard silica gel 60 (230–400 mesh) obtained from Merck. All products isolated were homogenous on TLC. Analytical high-performance liquid chromatography (HPLC) to determine the purity of the final compounds was performed using a Waters 2487 Dual Wavelength Absorbance detector, a Waters 1525 binary HPLC pump, a Waters In-Line Degasser AF, a Waters 717plus Autosampler and a Varian Pursuit XRs C18 reverse phase 150 × 4.6 mm chromatography column. Samples were detected using a wavelength of 254 nm. All samples were analysed using acetonitrile (70%): water (30%) over 10 min with a flow rate of 1 mL/min. Unless otherwise indicated, the purity of the final products was ≥95%. Analyses indicated by the symbols of the elements or functions were within ±0.4% of the theoretical values.

*4.1.1. General preparation of Schiff bases (**14**–**25**)*

A solution of the appropriately substituted aryl aldehyde (0.1 mol) and the appropriately substituted aryl amine (0.1 mol) in ethanol (50 mL) was heated at reflux for three hours. The reaction mixture was reduced to 25 mL under vacuum. The mixture was left to stand and the Schiff base product crystallized out of the solution. The crude product was then recrystallized from ethanol and filtered to yield the purified product. Schiff bases **15**, **17**, **19**, **20** and **25** were prepared and isolated as previously reported [14].

N-(4-Ethoxybenzylidene)-3,4,5-trimethoxyaniline **14**. Preparation was as above from 3,4,5-trimethoxybenzenamine and 4-

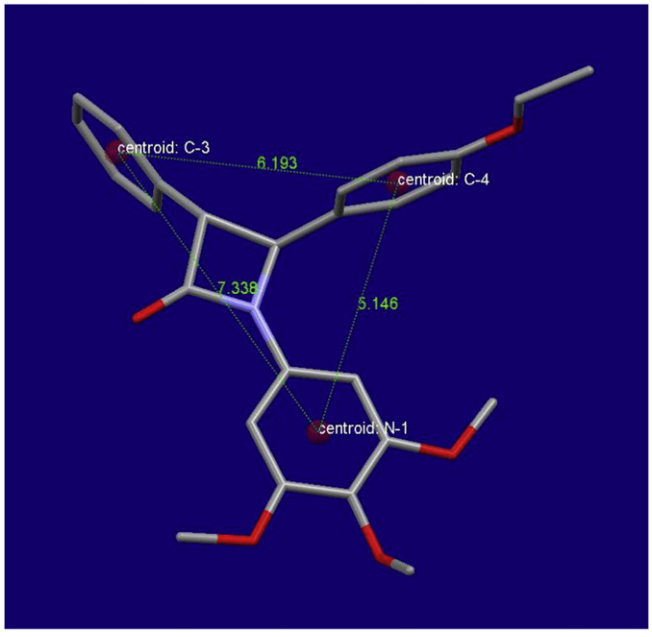

Fig. 8. Distances between the centres of the three phenyl rings of β-lactam **26** (single crystal X-ray structure).

ethoxybenzaldehyde. Yield 64%, yellow crystalline solid, m.p. 98 °C. IR ν_{max} (KBr): 1604.72 cm^{-1}, 1586.85 cm^{-1} (−C═N−). ^1H NMR (400 MHz, $CDCl_3$) δ 1.43−1.47 (t, 3H), 3.86 (s, 3H), 3.90 (s, 6H), 4.08−4.13 (m, 2H), 6.47 (s, 2H), 6.97 (d, 2H, $J = 8.28$ Hz), 7.83 (d, 2H, $J = 8.8$ Hz), 8.40 (s, 1H). ^{13}C NMR (100 MHz, $CDCl_3$) δ 14.30, 55.65, 60.58, 63.22, 97.63, 114.23, 128.42, 130.03, 135.58, 147.90, 153.08, 158.74, 161.26. Elemental analysis: $C_{18}H_{21}NO_4$ (C, H, N).

N-(4-(Dimethylamino)benzylidene)-3,4,5-trimethoxyaniline **16**. Preparation was as above from 4-dimethylaminobenzaldehyde and 3,4,5-trimethoxyaniline. Yield 64%, yellow crystals, m.p. 83−84 °C. IR ν_{max} (KBr): 1602.7 cm^{-1} (C═N). ^1H NMR (400 MHz, $CDCl_3$): δ 3.08 (s, 6H, −N−CH_3), 3.85 (s, 3H OCH_3), 3.89 (s, 6H, OCH_3), 6.47 (s, 2H, ArH), 6.73 (d, 2H, $J = 9$ Hz, ArH), 7.76 (d, 2H, $J = 9.04$ Hz, ArH), 8.33 (s, 1H, −CH═N). ^{13}C NMR (100 MHz, $CDCl_3$): δ 39.42, 55.42, 55.61, 60.54, 97.64, 111.10, 123.54, 130.01, 135.14, 148.42, 152.08, 152.99, 159.43. HRMS: Calculated for $C_{18}H_{23}N_2O_3$: 314.3790; Found 315.1709 ($M^+ + H$).

3,4,5-Trimethoxy-N-(2,4,6-trimethoxybenzylidene)aniline **18**. Preparation was as above from 2,4,6-trimethoxybenzaldehyde and 3,4,5-trimethoxyaniline. Yield 69%, Orange gel, IR ν_{max} (NaCl film): 1659.4 cm^{-1} (C═N). ^1H NMR (400 MHz, $CDCl_3$): δ 3.86 (s, 3H, OCH_3), 3.90 (s, 9H, OCH_3), 3.94 (s, 3H, OCH_3), 3.96 (s, 3H, OCH_3), 6.48 (s, 2H, ArH), 6.52 (s, 1H, ArH), 7.65 (s, 1H, ArH), 8.82 (s, 1H, −CH═N). ^{13}C NMR (100 MHz, $CDCl_3$): δ 56.01, 56.22, 56.38, δ 60.95, 98.20, 108.84, 116.48, 136.78, 143.55, 148.87, 153.37, 155.04, 155.16.

N-(3-Bromo-4-methoxybenzylidene)-3,4,5-trimethoxyaniline **21**. Preparation was as above from 3,4,5-trimethoxyaniline and 3-bromo-4-methoxybenzaldehyde. Yield 68%, Yellow crystalline solid, m.p. 128 °C. IR ν_{max} (KBr): 1620.47 cm^{-1}, 1585.77 cm^{-1} (−C═N−). ^1H NMR (400 MHz, $CDCl_3$) δ 3.89 (s, 3H), 3.92 (s, 6H), 3.99 (s, 3H), 6.50 (s, 2H), 7.00 (d, 1H, $J = 8.52$ Hz), 7.79−7.81 (dd, 1H), 8.18 (d, 1H, $J = 2$ Hz), 8.38 (s, 1H). ^{13}C NMR (100 MHz, $CDCl_3$) δ 55.68, 56.00, 60.59, 97.67, 111.13, 111.95, 129.22, 129.81, 132.82, 135.92, 147.24, 153.13, 157.00, 157.81. HRMS: $C_{17}H_{18}NO_4Br$ requires 380.0580; found 380.0497; elemental analysis: $C_{17}H_{18}BrNO_4$ (C, H, N, Br).

3,4,5-Trimethoxy-N-(naphthalen-2-ylmethylene)aniline **22**. Preparation was as above from 2-naphthaldehyde and 3,4,5-trimethoxyaniline. Yield 77%, yellow crystals, m.p. 108−116 °C. IR ν_{max} (KBr): 1625.74, 1610.62 and 1583.40 cm^{-1} (C═N).δ 3.88 (s, 6H, OCH_3), 3.93 (s, 3H, OCH_3), 6.57−7.25 (m, 9H, ArH), 8.67 (s, 1H, N═CH). Elemental analysis: $C_{20}H_{19}NO_3$ (C, H, N).

3,4,5-Trimethoxy-N-(3-(4-methoxyphenyl)allylidene)aniline **23**. Preparation was as above from 3-(4-methoxyphenyl)propenal and 3,4,5-trimethoxyaniline. Yield 57%, Yellow crystalline solid, m.p. 128 °C. IR ν_{max} (NaCl): 1626.36 cm^{-1}, 1582.90 cm^{-1} (−C═N−). ^1H NMR (400 MHz, CDCl3) δ 3.86−3.90 (m, 12H), 6.48 (s, 2H), 6.93−7.02 (m, 3H), 7.12−7.16 (m, 1H), 7.50 (d, 1H, $J = 9.04$ Hz), 8.28 (d, 1H, $J = 9.04$ Hz). HRMS: $C_{19}H_{22}NO_4$ requires 328.1549; found 328.1545 ($M^+ + H$).

N-(4-Methoxybenzylidene)-1-(3,4,5-trimethoxyphenyl)methanamine **24**. Preparation was as above from 3,4,5-trimethoxybenzylamine and 4-methoxybenzaldehyde. Yield 54%, Colourless crystals, m.p. 62 °C. IR ν_{max} (KBr): 1630.82, 1603.44 cm^{-1}. ^1H NMR (400 MHz, $CDCl_3$) δ 3.85−3.88 (m, 12H), 4.74 (s, 2H), 6.60 (s, 2H), 6.97 (d, 2H, $J = 9.04$ Hz), 7.76 (d, 2H, $J = 8.52$ Hz), 8.35 (s, 1H). ^{13}C NMR (100 MHz, $CDCl_3$) δ 54.93, 55.63, 55.69, 60.39, 64.82, 76.31, 76.63, 76.95, 103.46, 104.44, 113.56, 113.86, 128.55, 129.43, 131.56, 134.87, 136.41, 152.83, 160.87, 161.33. Elemental analysis: $C_{18}H_{21}NO_4$ (C, H, N).

4.1.2. General methods for preparation of 3-substituted azetidin-2-ones

4.1.2.1. Staudinger reaction (method I). A solution consisting of acetyl chloride (7.5 mmol) in anhydrous CH_2Cl_2 (50 mL) was added dropwise to a stirring solution containing the appropriate imine (5 mmol) and triethylamine (15 mmol) in anhydrous CH_2Cl_2 (50 mL) at reflux in an inert atmosphere. The solution was refluxed for 10 hours and then washed with saturated sodium bicarbonate solution (50 mL), dilute (10%) HCl (50 mL) and brine (50 mL). The organic layer was dried and evaporated *in vacuo*.

4.1.2.2. Modified Staudinger reaction (method II). The appropriate imine (10 mmol) and acetyl chloride (10 mmol) were added to anhydrous CH_2Cl_2 (50 mL) under nitrogen and the mixture was left stirring for 2 h. Triethylamine (10 mmol) was injected dropwise and the mixture was stirred overnight. The mixture was washed with distilled water (50 mL) (twice) and then with saturated aqueous sodium bicarbonate solution (50 mL). The organic layer was dried by filtration through anhydrous sodium sulfate. The organic layer containing the product was collected and reduced *in vacuo*.

4-(4-Fluorophenyl)-3-phenyl-1-(3,4,5-trimethoxyphenyl)azetidin-2-one **27**. Preparation was from **15** (5 mmol) as described in method I. Evaporation of solvent yielded a brown solid residue which was purified using column chromatography hexane:diethyl ether (1:1). Yield 11%, Orange gel. IR ν_{max} (KBr): 1706.1 cm^{-1} (C═O, β-lactam). ^1H NMR (400 MHz, $CDCl_3$): δ 3.72 (s, 6H, OCH_3), 3.78 (s, 3H, OCH_3), 4.26−4.27 (d, 1H, $J = 2.5$ Hz, H_3), 4.91−4.92 (d, 1H, $J = 2.5$ Hz, H_4), 6.61 (s, 2H, ArH), 7.14 (m, 2H, ArH), 7.31−7.45 (m, 7H, ArH). ^{13}C NMR (100 MHz, $CDCl_3$): δ 55.57, 60.51, 62.98, 64.66, 94.35, 115.86, 116.07, 126.97, 128.68, 132.80, 133.05, 133.99, 134.17, 153.15, 163.62, 164.88. HRMS: $C_{24}H_{22}FNO_4Na$ requires 430.1430; found 430.1395 ($M^+ + Na$).

4-(4-(Dimethylamino)phenyl)-3-phenyl-1-(3,4,5-trimethoxyphenyl) azetidin-2-one **28**. Preparation was from **16** (10 mmol) as described in method I. Evaporation of solvent yielded a brown solid residue which was purified using column chromatography hexane:diethyl ether (1:1). Yield 6%, Orange powder, m.p. 118 °C. IR ν_{max} (NaCl film): 1745.1 cm^{-1} (C═O, β-lactam). ^1H NMR (400 MHz, $CDCl_3$): δ 2.99 (s, 6H, N-CH_3), 3.75 (s, 6H, OCH_3), 3.80 (s, 3H, OCH_3), 4.33 (d, 1H, $J = 2.5$ Hz, H_3), 4.86, (d, 1H, $J = 2.5$ Hz, H_4), 6.69 (s, 2H, ArH), 6.76 (d, 2H, $J = 8.5$ Hz, ArH), 7.31−7.33 (m, 2H, ArH), 7.35−7.39 (m, 5H, ArH). ^{13}C NMR (100 MHz, $CDCl_3$): δ 9.96, 55.55, 55.61, 60.49, 63.81, 64.42, 94.45, 112.26, 123.75, 126.74, 127.32, 127.52, 128.11, 128.32, 128.78, 129.19, 133.51, 134.21, 134.65, 150.34, 153.00, 153.21, 165.59. HRMS: $C_{26}H_{30}N_2O_4$ requires 433.5116; found 433.2112 ($M^+ + H$).

3-Phenyl-4-(2,3,4-trimethoxyphenyl)-1-(3,4,5-trimethoxyphenyl) azetidin-2-one **29**. Preparation was from **17** (3 mmol) as described in method I. Evaporation of solvent yielded a brown solid residue, which was purified using column chromatography hexane:diethyl ether (1:1). Yield 10%, Yellow solid, m.p. 92 °C. IR ν_{max} (NaCl film): 1749.2 cm^{-1} (C═O, β-lactam). ^1H NMR (400 MHz, $CDCl_3$): δ 3.74 (s, 6H, OCH_3), 3.77 (s, 3H, OCH_3), 3.80 (s, 3H, OCH_3), 3.86 (s, 3H, OCH_3), 3.88 (s, 3H, OCH_3). δ 4.36 (d, 1H, $J = 2.5$ Hz, H_3), 5.22 (d, 1H, $J = 2.5$ Hz, H_4), 6.63 (s, 2H, ArH), 7.05 (d, 1H, $J = 8.6$ Hz, ArH), 7.15 (d, 1H, $J = 6.5$ Hz, ArH), δ 7.25−7.35 (m, 5H, ArH). ^{13}C NMR (100 MHz, $CDCl_3$): δ 55.56, 58.11, 60.40, 60.51, 61.12, 63.39, 94.30, 107.34, 121.07, 126.59, 127.02, 127.30, 128.24, 128.76, 129.58, 130.18, 133.31, 134.55, 135.49, 153.07, 153.60, 160.03, 161.70, 165.46. HRMS: $C_{27}H_{29}NO_7Na$ requires 502.1842; found 502.1823 ($M^+ + Na$).

3-Phenyl-4-(2,4,6-trimethoxyphenyl)-1-(3,4,5-trimethoxyphenyl) azetidin-2-one **30**. Preparation was from **18** (3 mmol) as described in method I. Evaporation of solvent yielded a brown solid residue, which was purified using column chromatography, hexane:diethyl ether (1:1). Yield 52%, Yellow solid, m.p. 112−114 °C. IR ν_{max} (KBr): 1746.6 cm^{-1} (C═O, β-lactam). ^1H NMR (400 MHz, $CDCl_3$): δ 3.73 (s, 3H, OCH_3), 3.75 (s, 3H, OCH_3), 3.81 (s, 3H, OCH_3), 3.85 (s, 3H, OCH_3), 3.86 (s, 6H, OCH_3), 4.86 (d, 1H, $J = 2.5$ Hz, H_3), 5.52 (d, 1H, $J = 2.5$ Hz, H_4), 6.07 (s, 2H, ArH), 6.64 (s, 2H, ArH), 7.34−7.37 (m, 5H, ArH). ^{13}C

NMR (100 MHz, $CDCl_3$): δ 54.44, 54.89, 55.05, 55.27, 55.48, 55.51, 58.88, 60.42, 89.76, 90.38, 93.72, 105.11, 126.83, 127.09, 128.29, 133.76, 136.13, 152.83, 159.86, 161.36, 163.83, 165.83.

3-Phenyl-1,4-bis(3,4,5-trimethoxyphenyl)azetidin-2-one **31**. Preparation was from **25** (3 mmol) as described in method I. Evaporation of solvent yielded a brown solid residue, which was purified using column chromatography, DCM:EtOAc (19:1). Yield 7%, Yellow powder, m.p. 231 °C. IR ν_{max} (KBr): 1747.2 cm^{-1} (C═O, β-lactam). ^1H NMR (400 MHz, $CDCl_3$): δ 3.74 (s, 6H, OCH_3), 3.79 (s, 3H, OCH_3), 3.83 (s, 6H, OCH_3), 3.87 (s, 3H, OCH_3), 4.31 (d, 1H, $J = 2.5$ Hz, H_3), 4.81 (d, 1H, $J = 2.5$ Hz, H_4), 6.62 (d, 4H, $J = 5$ Hz, ArH), 7.34–7.39 (m, 5H, ArH). ^{13}C NMR (100 MHz, $CDCl_3$): δ 55.60, 55.87, 60.47, 60.53, 64.10, 64.48, 94.42, 102.28, 127.03, 127.58, 128.25, 128.66, 129.05, 133.26, 134.17, 134.19, 153.09, 153.59, 165.20. HRMS: $C_{27}H_{29}NO_7Na$ requires 502.1842; Found 502.1849 ($M^+ + Na$).

3-Phenyl-4-(2,4,5-trimethoxyphenyl)-1-(3,4,5-trimethoxyphenyl) azetidin-2-one **32**. Preparation was from **19** (4 mmol) as described in method I. Evaporation of solvent yielded a brown solid residue, which was purified using column chromatography, DCM. Yield 6%, Yellow powder, m.p. 126–128 °C. IR ν_{max} (NaCl film): 1740.0 cm^{-1} (C═O, β-lactam). ^1H NMR (400 MHz, $CDCl_3$): δ 3.74 (s, 6H, OCH_3), 3.77 (d, 6H, $J = 4.52$ Hz, OCH_3), 3.82 (s, 3H, OCH_3), 3.91 (s, 3H, OCH_3), 4.40 (d, 1H, $J = 2$ Hz, H_3), 5.31 (d, 1H, $J = 2$ Hz, H_4), 6.58 (s, 1H, ArH), 6.66 (s, 2H, ArH), 6.85 (s, 1H, ArH), 7.27–7.35 (m, 5H, ArH). ^{13}C NMR (100 MHz, $CDCl_3$): δ 55.54, 55.60, 56.02, 56.31, 57.59, 60.52, 61.11, 62.84, 94.25, 96.93, 110.05, 115.65, 126.65, 127.73, 128.23, 129.83, 133.39, 133.92, 134.01, 143.15, 149.56, 151.50, 153.03, 165.64. HRMS: $C_{27}H_{29}NO_7Na$ requires 502.1842; Found 502.1835 ($M^+ + Na$).

4-(3,4-Dimethoxyphenyl)-3-phenyl-1-(3,4,5-trimethoxyphenyl) azetidin-2-one **33**. Preparation was from **20** (4 mmol) as described in method I. Evaporation of solvent yielded a brown solid residue, which was purified using column chromatography, DCM:EtOAc (19:1). Yield 5%, Orange solid, m.p. 106–108 °C. IR ν_{max} (NaCl film): 1738.9 cm^{-1} (C═O, β-lactam). ^1H NMR (400 MHz, $CDCl_3$): δ 3.72 (s, 6H, OCH_3), 3.78 (s, 3H, OCH_3), 3.85 (s, 3H, OCH_3), 3.89 (s, 3H, OCH_3), 4.31 (d, 1H, $J = 2.5$ Hz, H_3), 4.86 (d, 1H, $J = 2.5$ Hz, H_4), 6.63 (s, 2H, ArH), 6.89–6.91 (m, 2H, ArH), 6.99–7.01 (q, 1H, $J = 2$ Hz, 6 Hz, ArH), 7.31–7.40 (m, 5H, ArH). ^{13}C NMR (100 MHz, $CDCl_3$): δ 55.58, 60.44, 63.68, 64.47, 94.34, 107.90, 111.01, 118.31, 126.94, 127.43, 128.56, 129.31, 133.27, 134.23, 148.94, 149.32, 153.01, 165.21. HRMS: $C_{26}H_{27}NO_6Na$ requires 472.1736; found 472.1752 ($M^+ + Na$).

4-(3-Bromo-4-methoxyphenyl)-3-phenyl-1-(3,4,5-trimethoxyphenyl) azetidin-2-one **34**. Preparation was from **21** as described in method II. Yield 3.7%, Light off-white powder, m.p. 82 °C. IR ν_{max} (KBr): 1751.57 cm^{-1} (C═O, β-lactam). ^1H NMR (400 MHz, $CDCl_3$) δ 3.77 (s, 6H, OCH_3), 3.81 (s, 3H, OCH_3), 3.94 (s, 3H, OCH_3), 4.29 (d, 1H, $J = 2$ Hz), 4.85 (d, 1H, $J = 2$ Hz), 6.61 (s, 2H, ArH), 6.97 (s, 1H, ArH), 7.34–7.41 (m, 6H, ArH), 7.64 (s, 1H, ArH). ^{13}C NMR (400 MHz, $CDCl_3$) δ 55.65, 55.92, 60.53, 62.64, 64.65, 94.39, 111.98, 112.09, 125.68, 126.97, 127.63, 128.68, 130.47, 130.62, 133.03, 133.95, 153.16, 155.79, 164.89. HRMS: $C_{25}H_{24}BrNO_5$ requires 498.0916; found 498.0926 ($M^+ + H$).

4-(Naphthalen-2-yl)-3-phenyl-1-(3,4,5-trimethoxyphenyl)azetidin-2-one **35**. Preparation was from **22** as described in method I. Yield 5.4%, IR ν_{max} (KBr): 1751.19 cm^{-1} (C═O, β-lactam). ^1H NMR (400 MHz, $CDCl_3$): δ 3.70–3.78 (9H, OCH_3), 4.41 (m, 1H, H_3), 5.11 (m, 1H, H_4), 6.61 (s, 2H, ArH), 7.29–7.96 (m, 12H, ArH). ^{13}C NMR (400 MHz, $CDCl_3$): δ 56.06, 60.96, 64.38, 65.06, 94.89, 122.96, 134.97, 153.59, 165.58. HRMS: $C_{28}H_{25}NO_4Na$ requires 462.1681; Found 462.1673 ($M^+ + Na$).

4-(4-Methoxystyryl)-3-phenyl-1-(3,4,5-trimethoxyphenyl)azetidin-2-one **36**. Preparation was from **23** as described in method I. Yield 6%, Yellow oil. IR ν_{max} (NaCl film): 1747.40 cm^{-1} (C═O, β-lactam). ^1H NMR (400 MHz, $CDCl_3$) δ 3.82–3.85 (m, 12H, OCH_3), 4.31 (d, 1H, $J = 1.5$ Hz, H_3), 4.58–4.60 (m, 1H, H_4), 6.26–6.32 (m, 1H, ArH), 6.81–6.85 (t, 3H), 6.90 (d, 2H, $J = 8.5$ Hz), 7.37–7.39 (m, 7H). ^{13}C NMR (400 MHz, $CDCl_3$) δ 54.91, 55.65, 60.57, 61.76, 63.28, 94.22, 113.76, 123.98, 127.06, 127.46, 127.80, 128.57, 133.86, 153.12, 164.73. HRMS: $C_{27}H_{27}NO_5Na$ requires 468.1787; found 468.1785 ($M^+ + Na$).

4-(4-Methoxyphenyl)-3-phenyl-1-(3,4,5-trimethoxybenzyl)azetidin-2-one **37**. Preparation was from **24** as described in method I. Yield 7.3%, Clear oil. IR ν_{max} (NaCl film): 1751.30 cm^{-1} (C═O, β-lactam). ^1H NMR (400 MHz, $CDCl_3$) δ 3.79 (m, 6H, OCH_3), 3.85 (s, 6H, OCH_3), 4.22 (d, 1H, $J = 2$ Hz), 4.36 (d, 1H, $J = 2$ Hz), 4.88 (d, 1H, $J = 15.0$ Hz), 6.41 (s, 2H), 6.96 (d, 2H, $J = 8.4$ Hz), 7.17–7.31 (m, 11H, ArH). ^{13}C NMR (400 MHz, $CDCl_3$) δ 21.49, 44.75, 55.39, 56.03, 60.88, 62.80, 65.03, 105.31, 114.50, 125.32, 127.33, 127.69, 127.93, 128.25, 128.92, 129.06, 131.34, 135.18, 137.32, 137.87, 153.43, 159.98, 168.45. HRMS: $C_{26}H_{27}NO_5Na$ requires 456.1787; found 456.1798 ($M^+ + Na$).

4.1.2.3. Reformatsky microwave reaction (method III). For preparation of *4-(4-ethoxyphenyl)-3-phenyl-1-(3,4,5-trimethoxyphenyl)azetidin-2-one* **26**. Zinc dust (6.9 mmol) was placed in 10 mL microwave vial and 5 mL of anhydrous benzene was added and the vial capped. TMCS (0.325 mL) was added. The reaction was stirred at 25 °C, 50 W, for 15 min and then heated at 100 °C, 200 W for 3 min. The vessel was allowed to cool before addition of N-(4-ethoxybenzylidene)-3,4,5-trimethoxyaniline **14** (5 mmol) and ethyl-α-bromophenylacetate (6 mmol). Reaction was carried out at 100 °C, 200 W, 30 min. It was then poured over 20 mL of saturated NH_4Cl and 20 mL of 25% NH_4OH. CH_2Cl_2 (20 mL) is used to extract the organic layer which is further washed with 20 mL 0.1 N HCl and 20 mL of water. The organic layer is separated and dried using anhydrous sodium sulfate. *4-(4-Ethoxyphenyl)-3-phenyl-1-(3,4,5-trimethoxyphenyl)azetidin-2-one* **26** was obtained in 7% yield as a white crystalline material, m.p. 109 °C. IR ν_{max} (KBr): 1754.92 cm^{-1} (C═O, β-lactam). ^1H NMR (400 MHz, $CDCl_3$) δ 1.41–1.44 (t, 3H, CH_2), 3.72 (s, 6H, OCH_3), 3.77 (s, 3H, OCH_3), 4.28 (d, 1H, $J = 2$ Hz, H_3), 4.86 (d, 1H, $J = 2$ Hz, H_4), 6.60 (s, 2H, ArH), 6.93 (d, 2H, $J = 8.52$ Hz), 7.32–7.40 (m, 7H). ^{13}C NMR (100 MHz, $CDCl_3$) δ 14.35, 55.56, 60.51, 63.13, 63.43, 64.58, 94.39, 114.74, 126.88, 126.98, 127.43, 128.58, 128.68, 133.31, 134.00, 134.36, 146.43, 153.05, 158.90, 165.22. HRMS: $C_{26}H_{27}NO_5Na$ requires 456.1787; found 456.1800 ($M^+ + Na$).

*4.1.2.4. General method for synthesis of 4-diphenyl substituted β-lactams **38**, **39** and **40**.* $TiCl_4$ (2.0 mmol, 1 M in CH_2Cl_2) was added to a solution of the appropriately substituted benzophenone (4.0 mmol) and trimethoxyaniline (4.0 mmol) in anhydrous toluene (40 mL). Tri-*n*-butylamine (12.2 mmol) was added. The resulting mixture was stirred overnight under nitrogen. Tri-*n*-butylamine (8.4 mmol) and phenylacetyl chloride (4.4 mmol) were added sequentially. The mixture was brought to reflux and refluxed for 8 h. The mixture was cooled to room temperature, the reaction was quenched with water, and the mixture was transferred to a separating funnel, diluted with ethyl acetate, washed with 1 M HCl, saturated $NaHCO_3$, water, and brine, dried over anhydrous sodium sulfate and purified using flash column chromatography over silica gel (eluent: hexane/ethyl gradient).

3,4,4-Triphenyl-1-(3,4,5-trimethoxyphenyl)azetidin-2-one **38**. Preparation was as above from benzophenone. Yield 0.4%, Yellow powder, m.p. 165 °C. IR ν_{max} (KBr): 1749.57 cm^{-1} (C═O, β-lactam). ^1H NMR (400 MHz, $CDCl_3$) δ 3.60 (s, 6H, OCH_3), 3.79 (s, 3H, OCH_3), 5.18 (s, 1H, H_3), 6.65 (s, 2H, ArH), 6.90–6.92 (m, 2H, ArH), 7.03–7.13 (m, 8H, ArH), 7.38–7.41 (m, 3H, ArH), 7.60–7.62 (m, 2H, ArH). ^{13}C NMR (100 MHz, $CDCl_3$) δ 55.88, 60.93, 72.44, 73.31, 95.97, 127.27, 127.46, 127.56, 127.94, 128.09, 128.50, 128.87, 129.21, 129.57, 132.79, 133.96, 134.21, 135.43, 140.56, 153.10, 166.61. HRMS: $C_{30}H_{27}NO_4Na$ requires 488.1838; found 488.1856 ($M^+ + Na$).

4-(4-Methoxyphenyl)-3,4-diphenyl-1-(3,4,5-trimethoxyphenyl) azetidin-2-one **39**. Preparation was as above from (4-methoxyphenyl)phenylmethanone. Yield 20%, White powder, m.p. 171 °C. IR ν_{max} (KBr): 1742.06 cm^{-1} (C═O, β-lactam). ^1H NMR (400 MHz, $CDCl_3$) δ 3.63 (s, 6H, OCH_3), 3.80 (s, 3H, OCH_3), 3.84 (s, 3H, OCH_3), 5.16 (s, 1H, H_3), 6.69 (s, 2H, ArH), 6.88–6.96 (m, 4H, ArH), 7.03–7.15 (m, 7H, ArH), 7.38–7.44 (m, 1H, ArH), 7.60 (d, 2H, $J = 8.8$ Hz, ArH). ^{13}C NMR (100 MHz, $CDCl_3$) δ 54.94, 55.45, 60.48, 72.02, 72.72, 95.50, 112.36, 113.62, 126.74, 126.97, 127.04, 127.40, 127.62, 127.70, 127.94, 128.38, 128.68, 128.87, 129.09, 129.94, 131.83, 132.44, 133.54, 133.72, 133.32, 152.64, 159.09, 166.26.

4,4-Bis-(4-methoxyphenyl)-3-phenyl-1-(3,4,5-trimethoxyphenyl) azetidin-2-one **40**. Preparation was as above from bis-(4-methoxyphenyl)methanone. Yield 17%, White powder, m.p. 165 °C. IR ν_{max} (KBr): 1742.60 cm^{-1} (C═O, β-lactam). ^1H NMR (400 MHz, $CDCl_3$) δ 3.63 (s, 6H, OCH_3), 3.73 (s, 3H, OCH_3), 3.80 (s, 3H, OCH_3), 3.84 (s, 3H, OCH_3), 5.12 (s, 1H, H_3), 6.63 (d, 2H, $J = 8.8$ Hz), 6.68 (s, 2H, ArH), 6.90–6.95 (m, 6H, ArH), 7.09–7.11 (s, 3H, ArH), 7.51 (d, 2H, $J = 9.28$ Hz, ArH). ^{13}C NMR (100 MHz, $CDCl_3$) δ 54.72, 54.94, 55.45, 60.48, 71.86, 72.31, 95.48, 112.31, 113.57, 127.04, 127.35, 127.67, 128.79, 129.08, 129.85, 132.22, 132.50, 133.55, 152.62, 158.05, 159.00, 166.34. HRMS: $C_{32}H_{31}NO_6Na$ requires 548.2049; found 548.2062 ($M^+ + Na$).

4.2. Biochemical evaluation of activity

4.2.1. Antiproliferative studies

All assays were performed in triplicate for the determination of mean values reported. Compounds were assayed as the free bases isolated from reaction. The human breast tumour cell line MCF-7 was cultured in Eagles minimum essential medium in a 95%O_2/5% CO_2 atmosphere with 10% fetal bovine serum, 2 mM L-glutamine and 100 μg/mL penicillin/streptomycin. The medium was supplemented with 1% non-essential amino acids. MDA-MB-231 cells were maintained in Dulbecco's Modified Eagle's medium (DMEM), supplemented with 10% (v/v) Fetal bovine serum, 2 mM L-glutamine and 100 μg/mL penicillin/streptomycin (complete medium). Cells were trypsinised and seeded at a density of 2.5×10^4 cells/mL in a 96-well plate and incubated at 37 °C, 95%O_2/5% CO_2 atmosphere for 24 h. After this time they were treated with 2 μL volumes of test compound which had been pre-prepared as stock solutions in ethanol to furnish the concentration range of study, 1 nM–100 μM, and re-incubated for a further 72 h. Control wells contained the equivalent volume of the vehicle ethanol (1% v/v). The culture medium was then removed and the cells washed with 100 μL phosphate buffered saline (PBS) and 50 μL MTT added, to reach a final concentration of 1 mg/mL MTT added. Cells were incubated for 2 h in darkness at 37 °C. At this point solubilization was begun through the addition of 200 μL DMSO and the cells maintained at room temperature in darkness for 20 min to ensure thorough colour diffusion before reading the absorbance. The absorbance value of control cells (no added compound) was set to 100% cell viability and from this graphs of absorbance versus cell density per well were prepared to assess cell viability and from these, graphs of percentage cell viability versus concentration of subject compound added were drawn.

4.2.2. Cytotoxicity

Cytotoxicity was determined using the CytoTox 96 non-radioactive cytotoxicity assay by Promega following the manufacturer's protocol [39]. The assay quantitatively measures lactate dehydrogenase (LDH) a stable cytosolic enzyme that is released upon cell lysis. Released LDH in culture supernatant is measured in a 30 min coupled enzymatic assay, which results in the conversion of a tetrazolium salt (INT) into a red formazan product [40].

MCF-7 and MDA-MB-231 cells were seeded in 96-well plates, incubated for 24 h and then treated with compounds as described for the antiproliferative assay above. After 72 h, 20 μL of lysis solution (10×) was added to the 'blank' wells and left for 1 h to ensure 100% death. A total of 50 μL was removed from each well and transferred to a new 96-well plate. A total of 50 μL of substrate mix from the LDH assay kit was added and the plate was incubated in the dark at room temperature for 30 min. After this period, 50 μL of stop solution was added to each well before reading the absorbance at a wavelength of 490 nm using a Dynatech MR5000 plate reader. Percentage cell death was calculated at 10 μM.

4.2.3. Tubulin polymerization assay

The effect of a selected analogue **26** on the polymerization of purified bovine brain tubulin was determined spectrophotometrically by monitoring the change in turbidity. Lyophilised tubulin (Cytoskeleton, Denver, CO) was re-suspended in ice cold G-PEM buffer (80 mM PIPES pH 6.9, 0.5 mM $MgCl_2$, 1 mM EGTA, 1 mM GTP, 10.2% (v/v) glycerol) and added to wells on a half volume 96-well plate containing the designated concentration of drug (10 μM) or vehicle. Samples were mixed well and tubulin assembly was monitored at A_{340nm} at 30 s intervals for 60 min at 37 °C in a Spectramax 340PC spectrophotometer (Molecular Devices).

4.2.4. Immunofluorescence and confocal microscopy

For immunofluorescence, MCF-7 cells were seeded at 1×10^5 per well on BD falcon four well chamber glass slides (BD Biosciences, San Jose, USA). Cells were treated with vehicle [1% ethanol (v/v)], **4** [100 nM], **26** [500 nM] for 16 h. Following treatment cells were washed gently in PBS, permabilised with PBS and 0.1% Triton-X-100, fixed for 30 min in methanol at −20 °C. Following washes in PBS cells were blocked in 5% BSA diluted in PBST (blocking buffer). Cells were then incubated with mouse anti-tubulin (DM1A (Merck Chemicals Ltd)); 1:20 for 1 h at room temperature. Following washes in PBST cells were incubated with fluorescein isothiocyanate (FITC) conjugated rabbit anti-mouse (Dakocytomation, UK); 1:200 for 1 h at room temperature. Following washes in PBST, the cells were mounted in Ultra Cruz Mounting Media (Santa Cruz Biotechnology, Santa Cruz, CA) containing 4,6-diamino-2-phenolindol dihydrochloride (DAPI). Confocal images were captured using the OLYMPUS 1X81 microscope coupled with OLYMPUS FLUOVIEW Ver 1.5 software. All images in each experiment were collected on the same day using identical parameters.

4.2.5. Determination of DNA content by flow cytometry

MCF-7 cells were seeded at 5×10^5 cells/mL in T25 flasks. After 24 h, cells were treated with vehicle [1% ethanol (v/v)], **4** [100 nM] or **26** [500 nM] for 48 h. Cells were harvested by centrifugation at $800 \times g$ for 10 min. Cell pellets were re-suspended in PBS and fixed in 70% ethanol: PBS overnight at −20 °C. Following centrifugation cell pellets were re-suspended in PBS supplemented with 0.5 mg/mL RNase and 0.15 mg/mL propidium iodide (PI). Following a 30-min incubation at 37 °C in the dark the PI fluorescence was measured on a linear scale using a FACSCalibur flow cytometer (Becton Dickinson, San Jose, CA). The amount of PI fluorescence is directly proportional to the amount of DNA present in each cell. The relative content of DNA indicates the distribution of a population of cells throughout the cell cycle. For example, cells in G_0G_1 are diploid and have a DNA content of 2N. Cells with the G_2M phases have a DNA content of 4N, while cells in S-phase have a DNA content between 2N and 4N. Apoptotic cells are sub-diploid (<2N). Data collection was gated to exclude cell debris and cell aggregates. At least 10,000 cells were analysed per sample. All data were recorded and analysed using the CellQuest software (Becton Dickinson).

4.3. X-ray crystallography

The X-ray crystallography data for compound **26** was collected on a Rigaku Saturn 724 CCD Diffractometer. A suitable crystal was selected and mounted on a glass fiber tip and placed on the goniometer head in a 123K N2 gas stream. The data set was collected using Crystalclear-SM 1.4.0 software and 1680 diffraction images, of 0.5° per image, were recorded. Data integration, reduction and correction for absorption and polarization effects were all performed using Crystalclear-SM 1.4.0 software. Space group determination, structure solution and refinement were obtained using Crystal structure ver. 3.8 and Bruker Shelxtl Ver. 6.14 software [41]. **Crystal Data for 26:** $C_{208}H_{216}N_8O_{40}$, MW3469.89 (unit cell), Monoclinic, Space group C2/c; $a = 20.90(3)$, $b = 17.62(2)$, $c = 14.02(2)$Å, $\beta = 119.95(5)$; $U = 4474(12)$(Å)^3; $Z = 1$; $Dc = 1.287$ mg m^{-3}; $m = 0.089$ mm^{-1}; Range for data collection = 2.12–25.00; Reflections collected 16136 , Unique Reflections 3934 [$R_{int} = 0.165$]; Data/restraints/parameters 3934/0/294; Goodness-of-fit on F2 1.194; R indices (all data) = $R_1 = 0.0746$, w$R_2 = 0.1678$; Final R indices [$I > 2s(I)$] = $R1 = 0.0646$, w$R_2 = 0.1596$. Cambridge Crystallographic Data Centre (CCDC ID: 815023).

4.4. Molecular modelling

PDB entry 1SA0 [36] was downloaded and only chains A and B with co-crystallized N-deacetyl-N-(2-mercaptoacetyl)-colchicine (DAMA-colchicine, **41**) were retained. The X-ray co-ordinates of compound **26** were used as input for a docking simulation carried out using Molegro Virtual Docker [42]. A search space of 15 Å around colchicine was created and the binding site defined by cavity detection within Molegro. No docking template was used to prevent search bias. A grid resolution of 0.30 Å and searching and scoring using MolDock score was enabled for 10 runs. All other parameters were kept as default and 10 poses were generated for each run. The top scoring docked solution was retained for analysis in MOE [43].

Acknowledgements

Sincere thanks to Dr. Gavin Mc Manus (School of Biochemistry and Immunology, TCD) for his technical assistance on the confocal microscope. A Trinity College Dublin postgraduate research studentship (Code 1252) and a one-year postgraduate research award for continuing students (Code 7017) are gratefully acknowledged. Support from the Health Research Board is also gratefully acknowledged.

References

[1] K.H. Downing, Structural basis for the interaction of tubulin with proteins and drugs that affect microtubule dynamics, Annu. Rev. Cell Dev. Biol. 16 (2000) 89.
[2] C. Dumontet, M.A. Jordan, Microtubule-binding agents: a dynamic field of cancer therapeutics, Nat. Rev. Drug Discovery 9 (2010) 790–803.
[3] British National Formulary, vol. 59, Pharmaceutical Press, Britain, 2010.
[4] G.M. Cragg, D.G. Kingston, D.J. Newman, Anticancer Agents from Natural Products. CRC Press, Florida, 2005.
[5] J.M. Watt, M. Gerdina, The Medicinal and Poisonous Plants of Southern and Eastern Africa. E. & S. Livingstone Ltd., Edinburgh and London, 1962.
[6] G.G. Dark, S.A. Hill, V.E. Prise, G.M. Tozer, G.R. Pettit, D.J. Chaplin, Combretastatin A-4, an agent that displays potent and selective toxicity toward tumor vasculature, Cancer Res. 57 (1997) 1829–1834.
[7] Available from: www.clinicaltrials.gov (Accessed 3 March 2011).
[8] K. Ohsumi, T. Hatanaka, R. Nakagawa, Y. Fukuda, Y. Morinaga, Y. Suga, Y. Nihei, K. Ohishi, Y. Akiyama, T. Tsuji, Synthesis and antitumor activities of amino acid prodrugs of amino-combretastatins, Anticancer Drug Des. 14 (1999) 539–548.
[9] L. Wang, K.W. Woods, Q. Li, K.J. Barr, R.W. McCroskey, S.M. Hannick, L. Gherke, R.B. Credo, Y.H. Hui, K. Marsh, R. Warner, J.Y. Lee, N. Zielinski-Mozng, D. Frost, S.H. Rosenberg, H.L. Sham, Potent, orally active heterocycle-based combretastatin A-4 analogues: synthesis, structure-activity relationship, pharmacokinetics, and in vivo antitumor activity evaluation, J. Med. Chem. 45 (2002) 1697–1711.
[10] K. Ohsumi, T. Hatanaka, K. Fujita, R. Nakagawa, Y. Fukuda, Y. Nihei, Y. Suga, Y. Morinaga, Y. Akiyama, T. Tsuji, Syntheses and antitumor activity of cis-restricted combretastatins: 5-membered heterocyclic analogues, Bioorg. Med. Chem. Lett. 8 (1998) 3153–3158.
[11] I. Barrett, M. Carr, N. O'Boyle, L.M. Greene, A.J.S. Knox, D.G. Lloyd, D.M. Zisterer, M.J. Meegan, Lead identification of conformationally restricted benzoxepin type combretastatin analogs: synthesis, antiproliferative activity, and tubulin effects, J. Enzyme Inhib. Med. Chem. 25 (2010) 180–194.
[12] P.D. Mehta, N.P.S. Sengar, A.K. Pathak, 2-Azetidinone – a new profile of various pharmacological activities, Eur. J. Med. Chem. 45 (2010) 5541–5560.
[13] L. Sun, N.I. Vasilevich, J.A. Fuselier, S.J. Hocart, D.H. Coy, Examination of the 1,4-disubstituted azetidinone ring system as a template for combretastatin A-4 conformationally restricted analogue design, Bioorg. Med. Chem. Lett. 14 (2004) 2041–2046.
[14] M. Carr, L.M. Greene, A.J.S. Knox, D.G. Lloyd, D.M. Zisterer, M.J. Meegan, Lead identification of conformationally restricted beta-lactam type combretastatin analogues: synthesis, antiproliferative activity and tubulin targeting effects, Eur. J. Med. Chem. 45 (2010) 5752–5766.
[15] N.M. O'Boyle, M. Carr, L.M. Greene, O. Bergin, S.M. Nathwani, T. McCabe, D.G. Lloyd, D.M. Zisterer, M.J. Meegan, Synthesis and evaluation of azetidinone analogues of combretastatin A-4 as tubulin targeting agents, J. Med. Chem. 53 (2010) 8569–8584.
[16] N.M. O'Boyle, L.M. Greene, O. Bergin, J.-B. Fichet, T. McCabe, D.G. Lloyd, D.M. Zisterer, M.J. Meegan, Synthesis, evaluation and structural studies of antiproliferative tubulin-targeting azetidin-2-ones, Bioorg. Med. Chem. 19 (2011) 2306–2325.
[17] A.K. Bose, G. Spiegelman, M.S. Manhas, Studies on lactams. Part XVI. Stereochemistry of [beta]-lactam formation, Tetrahedron Lett. 12 (1971) 3167–3170.
[18] G.I. Georg, The Organic Chemistry of Beta-Lactams. VCH Publishers, Inc., New York and Cambridge, 1992.
[19] I. Banik, F.F. Becker, B.K. Banik, Stereoselective synthesis of beta-lactams with polyaromatic imines: entry to new and novel anticancer agents, J. Med. Chem. 46 (2003) 12–15.
[20] G.S. Singh, Recent progress in the synthesis and chemistry of azetidinones, Tetrahedron 59 (2003) 7631–7649.
[21] J. March, in: Advanced Organic Chemistry. Reactions, Mechanisms and Structure, fourth ed. John Wiley & Sons, Inc., United States, 1992.
[22] T. Imamoto, N. Iwadate, K. Yoshida, Enantioselective hydrogenation of acyclic aromatic N-aryl imines catalyzed by an iridium complex of (S, S)-1,2-Bis(tert-butylmethylphosphino)ethane, Org. Lett. 8 (2006) 2289–2292.
[23] S.M.S. Joseph, E.B. Jan, Ruthenium-catalyzed transfer hydrogenation of imines by propan-2-ol in benzene, Chem. Eur. J. 8 (2002) 2955–2961.
[24] J.W. Clader, D.A. Burnett, M.A. Caplen, M.S. Domalski, S. Dugar, W. Vaccaro, R. Sher, M.E. Browne, H. Zhao, R.E. Burrier, B. Salisbury, H.R. Davis Jr., 2-Azetidinone cholesterol absorption inhibitors: structure–activity relationships on the heterocyclic nucleus, J. Med. Chem. 39 (1996) 3684–3693.
[25] T. Mosmann, Rapid colorimetric assay for cellular growth and survival: application to proliferation and cytotoxicity assays, J. Immunol. Methods 65 (1983) 55–63.
[26] N.H. Nam, Combretastatin A-4 analogues as antimitotic antitumor agents, Curr. Med. Chem. 10 (2003) 1697–1722.
[27] N.J. Lawrence, L.A. Hepworth, D. Rennison, A.T. McGown, J.A. Hadfield, Synthesis and anticancer activity of fluorinated analogues of combretastatin A-4, J. Fluorine Chem. 123 (2003) 101–108.
[28] G.R. Pettit, M.R. Rhodes, D.L. Herald, E. Hamel, J.M. Schmidt, R.K. Pettit, Antineoplastic agents. 445. Synthesis and evaluation of structural modifications of (Z)- and (E)-combretastatin A-4, J. Med. Chem. 48 (2005) 4087–4099.
[29] Y. Kong, J. Grembecka, M.C. Edler, E. Hamel, S.L. Mooberry, M. Sabat, J. Rieger, M.L. Brown, Structure-based discovery of a boronic acid bioisostere of combretastatin A-4, Chem. Biol. 12 (2005) 1007–1014.
[30] A.B.S. Maya, C. Perez-Melero, C. Mateo, D. Alonso, J.L. Fernandez, C. Gajate, F. Mollinedo, R. Pelaez, E. Caballero, M. Medarde, Further naphthylcombretastatins. An investigation on the role of the naphthalene moiety, J. Med. Chem. 48 (2005) 556–568.
[31] M. Castedo, J.-L. Perfettini, T. Roumier, K. Andreau, R. Medema, G. Kroemer, Cell death by mitotic catastrophe: a molecular definition, Oncogene 23 (2004) 2825–2837.
[32] S.M. Nabha, R.M. Mohammad, M.H. Dandashi, B. Coupaye-Gerard, A. Aboukameel, G.R. Pettit, A.M. Al-Katib, Combretastatin-A4 prodrug induces mitotic catastrophe in chronic lymphocytic leukemia cell line independent of caspase activation and poly(ADP-ribose) polymerase cleavage, Clinical Cancer Res. 8 (2002) 2735–2741.
[33] I. Vitale, A. Antoccia, C. Cenciarelli, P. Crateri, S. Meschini, G. Arancia, C. Pisano, C. Tanzarella, Combretastatin CA-4 and combretastatin derivative induce mitotic catastrophe dependent on spindle checkpoint and caspase-3 activation in non-small cell lung cancer cells, Apoptosis 12 (2007) 155–166.
[34] C. Cenciarelli, C. Tanzarella, I. Vitale, C. Pisano, P. Crateri, S. Meschini, G. Arancia, A. Antoccia, The tubulin-depolymerising agent combretastatin-4 induces ectopic aster assembly and mitotic catastrophe in lung cancer cells H460, Apoptosis 13 (2008) 659–669.

[35] D. Simoni, R. Romagnoli, R. Baruchello, R. Rondanin, M. Rizzi, M.G. Pavani, D. Alloatti, G. Giannini, M. Marcellini, T. Riccioni, M. Castorina, M.B. Guglielmi, F. Bucci, P. Carminati, C. Pisano, Novel combretastatin analogues endowed with antitumor activity, J. Med. Chem. 49 (2006) 3143–3152.
[36] R.B.G. Ravelli, B. Gigant, P.A. Curmi, I. Jourdain, S. Lachkar, A. Sobel, M. Knossow, Insight into tubulin regulation from a complex with colchicine and a stathmin-like domain, Nature 428 (2004) 198–202.
[37] J.M. Andreu, B. Perez-Ramirez, M.J. Gorbunoff, D. Ayala, S.N. Timasheff, Role of the colchicine ring A and its methoxy groups in the binding to tubulin and microtubule inhibition, Biochemistry 37 (1998) 8356–8368.
[38] F. Lara-Ochoa, G. Espinosa-Pérez, A new synthesis of combretastatins A-4 and AVE-8062A, Tetrahedron Lett. 48 (2007) 7007–7010.
[39] M.J. Allen, N. Rushton, Use of the CytoTox 96TM assay in routine biocompatibility testing in vitro, Promega Notes 45 (1994) 7–10.
[40] M.M. Nachlas, S.I. Margulies, J.D. Goldberg, A.M. Seligman, The determination of lactic dehydrogenase with a tetrazolium salt, Anal. Biochem. 1 (1960) 317–326.
[41] G.M. Sheldrick (Ed.), Software Reference Manual, SHELXTL, An Integrated System for Data Collection, Processing, Structure Solution and Refinement, Bruker Analytical X-Ray Systems Inc., Madison, WI, 2001.
[42] Molegro Virtual Docker v4.3.0, 2011. Available from: http://www.molegro.com.
[43] MOE, 2010, Chemical Computing Group, Available from: http://www.chemcomp.com/software.htm.
[44] J.P. Liou, Y.L. Chang, F.M. Kuo, C.W. Chang, H.Y. Tseng, C.C. Wang, Y.N. Yang, J.Y. Chang, S.J. Lee, H.P. Hsieh, Concise synthesis and structure-activity relationships of combretastatin A-4 analogues, 1-aroylindoles and 3-aroylindoles, as novel classes of potent antitubulin agents, J. Med. Chem. 47 (2004) 4247–4257.
[45] B.L. Flynn, G.P. Flynn, E. Hamel, M.K. Jung, The synthesis and tubulin binding activity of thiophene-based analogues of combretastatin A-4, Bioorg. Med. Chem. Lett. 11 (2001) 2341–2343.
[46] G. La Regina, T. Sarkar, R. Bai, M.C. Edler, R. Saletti, A. Coluccia, F. Piscitelli, L. Minelli, V. Gatti, C. Mazzoccoli, V. Palermo, C. Mazzoni, C. Falcone, A.I. Scovassi, V. Giansanti, P. Campiglia, A. Porta, B. Maresca, E. Hamel, A. Brancale, E. Novellino, R. Silvestri, New arylthioindoles and related bioisosteres at the sulfur bridging group. 4. Synthesis, tubulin polymerization, cell growth inhibition, and molecular modeling studies, J. Med. Chem. 52 (2009) 7512–7527.
[47] S. Messaoudi, B. Treguier, A. Hamze, O. Provot, J.-F. Peyrat, J.R. De Losada, J.-M. Liu, J. Bignon, J. Wdzieczak-Bakala, S. Thoret, J. Dubois, J.-D. Brion, M. Alami, Isocombretastatins A versus combretastatins A: the forgotten isoCA-4 isomer as a highly promising cytotoxic and antitubulin agent, J. Med. Chem. 52 (2009) 4538–4542.
[48] C. Mousset, A. Giraud, O. Provot, A. Hamze, J. Bignon, J.-M. Liu, S. Thoret, J. Dubois, J.-D. Brion, M. Alami, Synthesis and antitumor activity of benzils related to combretastatin A-4, Bioorg. Med. Chem. Lett. 18 (2008) 3266–3271.